

# Power Spectrum of Uplink Array Signals with Random Phase and Delay Errors

V. Vlnrotter<sup>1</sup>

Jet Propulsion Laboratory, California Institute of Technology  
4800 Oak Grove Dr.  
Pasadena, CA 91109  
(818) 354-2745  
Victor.A.Vlnrotter@jpl.nasa.gov

**Abstract:** Uplink Array signals emanating from different antennas must be compensated for Doppler and delay in order to achieve the  $N^2$  array gain predicted by theory. However compensation is never perfect, leaving residual errors that cause losses in array gain and degradation in signal quality. Here we develop a mathematical model for Uplink Array signals in the presence of phase and delay errors, similar to well-known multipath analyses but with features unique to this problem. The resulting losses and distortions are described, and the power spectral density of the array signal derived first conditioned on a given error vector, then averaged over distributions deemed suitable for Uplink Array applications. The impact of phase and delay errors on array gain and signal distortion are addressed, and the maximum data throughput is quantified in terms of the assumed error statistics.

## 1. Introduction

Uplink Arraying technology has been developed for NASA's Deep Space Network (DSN), enabling greater reach and data throughput for future NASA missions, including manned missions to Mars and exploratory missions to the outer planets, the Kuiper belt, and beyond. The DSN uplink arrays employ  $N$  microwave antennas transmitting at X-band (7.1 GHz) carriers to produce signals that add coherently at the spacecraft, providing a power gain of  $N^2$  over a single antenna. This gain can be traded off directly for higher data rate at a given distance, or provide a given data-rate for commands and software uploads at a distance  $N$  times greater than possible with a single antenna. The uplink arraying concept has been demonstrated using the three operational 34-meter antennas of the Apollo complex at Goldstone, CA, which were used to transmit coherently phased array signals to the EPOXI spacecraft. Both two-element and three-element uplink arrays have been demonstrated, and theoretical array gains of 6 dB and 9.5 dB, respectively, were experimentally verified [1]. In addition, planetary radar capability has also been demonstrated successfully using the Uplink Array to illuminate the planets Mercury and Venus, obtaining Doppler-delay images of both planets as described in [2].

---

<sup>1</sup> Author is with the Jet Propulsion Laboratory, California Institute of Technology.

Deep-space missions require the ability to command spacecraft after launch, during cruise and the encounter phase, in order to provide two-way communication and ranging. In addition, in-flight reconfiguration may be required to accommodate unforeseen changes in mission objectives. The use of antenna arrays enables much greater data-rates, greater effective operating distance, and cost-effective scaling for more demanding future missions through a highly flexible design philosophy, via the inherently parallel architecture of antenna arrays.

However, residual errors in carrier phase and modulation delay can lead to degradation in combined power and modulated signal fidelity, which ultimately limits the data throughput and decoding accuracy at the spacecraft. The modeling of residual phase and delay errors relevant to uplink arrays, and evaluation of their impact on the combined signal is the subject of this paper.

## 2. Mathematical Model of Uplink Array Signals: Unmodulated Carrier

Time-varying range differences due to geometry are the largest components of signal delay and phase variations. Phases and delays are estimated via ultra-precise predicts and real-time measurements, which however are subject to error. Small residual delay ( $\Delta$ ) and phase ( $\theta$ ) errors due to predict and equipment inaccuracies, thermal instabilities, and tropospheric variations lead to losses in the combined signal and also impacts its bandwidth.

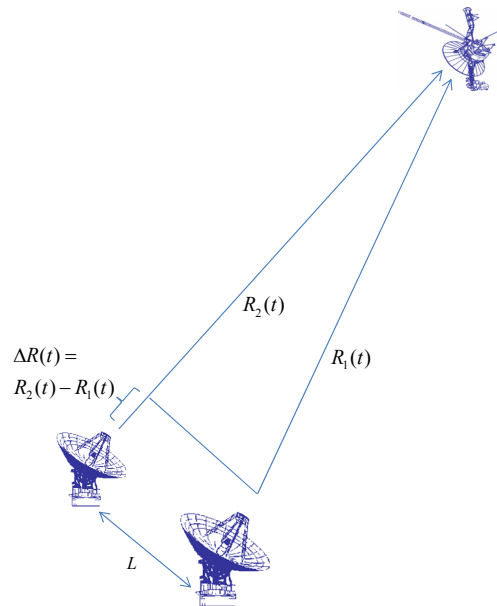


**Fig. 1 Two element Uplink Array geometry, defining the pathlength to the spacecraft at a particular time  $t$ ,  $R_1(t)$  and  $R_2(t)$ , and pathlength difference  $\Delta R(t)$ .**

It is convenient to represent the signal received at the spacecraft as the real part of the complex envelope,  $s(t) = \text{Re}\{\sqrt{2P}\tilde{s}_0(t)e^{j\omega t}\}$  where  $\tilde{s}_0(t) = d(t)e^{j\theta}$ ,  $d(t) = \pm 1$ , and define average power

$$|s(t)|^2 = \left( \text{Re} \left\{ \sqrt{2P} \tilde{s}_0(t) e^{j\omega t} \right\} \right)^2 = 2P d^2(t) \left( \text{Re} \left\{ e^{j(\omega t + \theta)} \right\} \right)^2 = 2P \cos^2(\omega t + \theta) = 2P \left\{ \frac{1}{2} [1 + \cos(2\omega t + 2\theta)] \right\}_{LP} = P$$

Alternately, we can define average power as the squared magnitude of the complex envelope, yielding the same model:

$$|s(t)|^2 = \left| \sqrt{P} \tilde{s}_0(t) e^{j\omega t} \right|^2 = P \left( d^2(t) e^{j\omega t} e^{-j\omega t} \right) = P \quad (1)$$

Clearly, the mathematical description is much simpler when the complex envelope model is employed, we therefore adopt this model.

Consider an Uplink Array of  $N$  elements, each radiating an unmodulated Doppler-compensated carrier at with random residual phase specified by the phase-vector  $\boldsymbol{\theta} = (\theta_1, \theta_2, \dots, \theta_N)$ . Each received complex signal at the spacecraft can be described in terms of a phasor-diagram, as shown in Figs. 2.

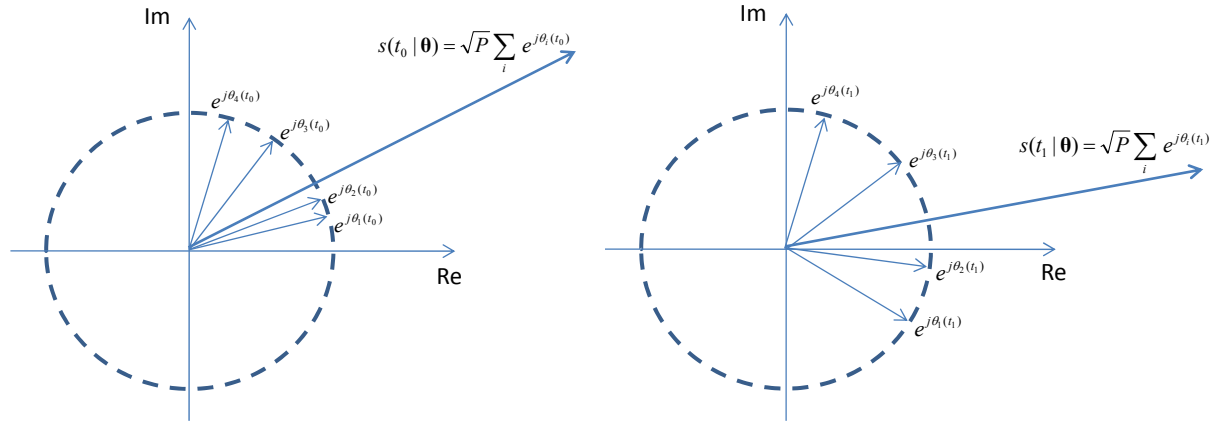


**Fig. 2. a) Phasor diagram of individual signals, and sum signal at the spacecraft, for a particular realization of the array phase-vector ; b) same, with a different realization of the array phase-vector.**

We shall make the realistic assumption that each component of the phase vector changes slowly enough so that a constant-phase assumption can be made over a suitably small time-interval, for purposes of analysis. With this model, Fig. 2a may describe the phase-vector at a particular time  $t_0$ , which may evolve with time to a different realization of the phase-vector at a later time  $t_1$ , as shown in Fig. 2b. At a given time  $t$ , the combined signal can be represented as the sum of the complex envelopes,

$s(t | \boldsymbol{\theta}) = \sqrt{P} \sum_i e^{j\theta_i(t)}$ , where each array element transmits  $P$  watts of power. The combined power at the spacecraft can then be expressed as the squared magnitude of the complex envelopes as

$$\begin{aligned}
|s(t|\boldsymbol{\theta})|^2 &= \left| \sqrt{P} \sum_{i=1}^N e^{j\theta_i(t)} \right|^2 = P \left( \sum_{i=1}^N \sum_{k=1}^N e^{j[\theta_i(t)-\theta_k(t)]} \right) \\
&= P \left( \sum_{i=1}^N e^{j[\theta_i(t)-\theta_i(t)]} + \sum_{i=1}^N \sum_{\substack{k=1 \\ k \neq i}}^N e^{j[\theta_i(t)-\theta_k(t)]} \right) = P \left( N + \sum_{i=1}^N \sum_{\substack{k=1 \\ k \neq i}}^N e^{j[\theta_i(t)-\theta_k(t)]} \right)
\end{aligned} \tag{2}$$

This model will be used to evaluate the average combined power at the spacecraft with various assumptions on the statistics of the phase components.

First consider a conventional derivation assuming statistically independent (SI), zero-mean Gaussian distributed phase vectors, which leads to accurate results when the variance of the phase error is vanishingly small. The Gaussian probability density for various values of  $\sigma_\theta^2$  is shown in Fig. 3, where it can be seen that for small variances it becomes a highly peaked function centered at zero phase.

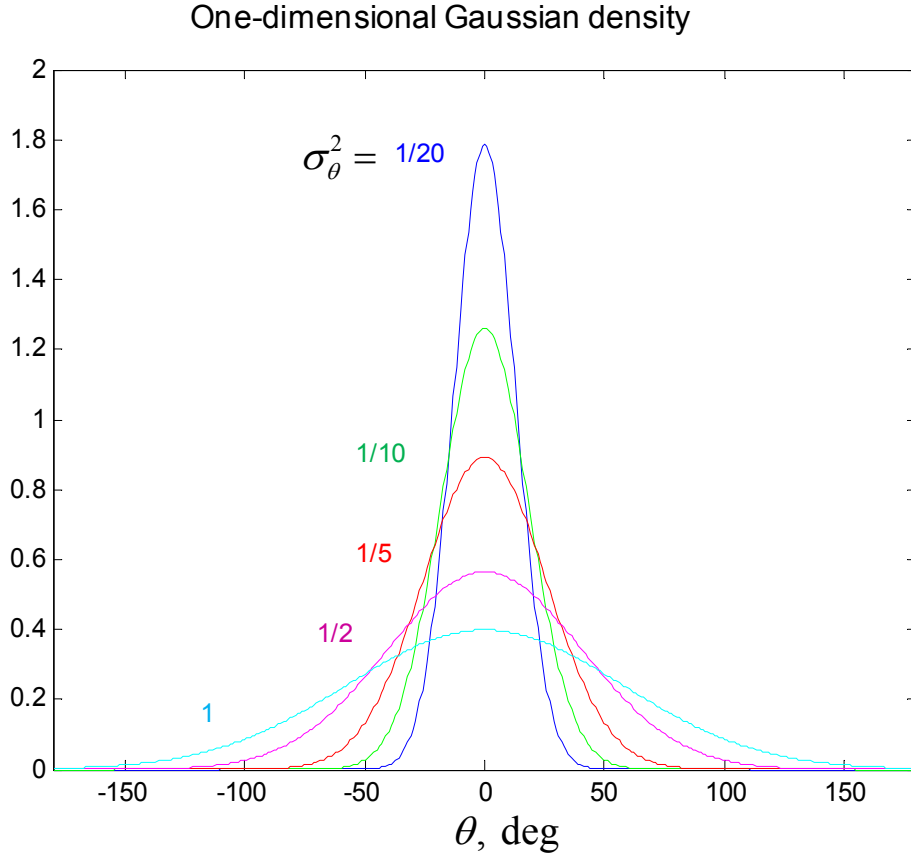


**Fig. 3. Zero-mean Gaussian probability density for variance of 1/20 and greater, showing peaked behavior for small  $\sigma_\theta^2$ .**

Let  $\theta_i$  and  $\theta_k$  be SI  $\forall i \neq k$ , and let  $p(\theta_i) = \frac{1}{\sqrt{2\pi\sigma_\theta^2}} e^{-\theta_i^2/2\sigma_\theta^2}$ , where  $\sigma_\theta^2$  is the variance of each.

The approach we take is to condition the combined power at the spacecraft on the random phase

vector, then average over the assumed phase statistics. Letting overbar denote averaging, and invoking the statistical independence of the phase components,  $\theta_i, \theta_k$  SI, the combined power can be expressed as

$$\overline{|s(t | \boldsymbol{\theta})|^2}^\theta = \overline{\left| \sqrt{P} \sum_{i=1}^N e^{j\theta_i(t)} \right|^2}^\theta = P \left( N + \sum_{i=1}^N \sum_{\substack{k=1 \\ k \neq i}}^N e^{j[\theta_i(t)]} e^{-j[\theta_k(t)]} \right)^\theta = P \left( N + \sum_{i=1}^N \sum_{\substack{k=1 \\ k \neq i}}^N \overline{e^{j[\theta_i(t)]}}^\theta \overline{e^{-j[\theta_k(t)]}}^\theta \right) \quad (3)$$

Averaging each component with respect to the Gaussian density yields [3]:

$$\overline{e^{\pm j\theta}}^\theta = \frac{1}{\sqrt{2\pi\sigma_\theta^2}} \int_{-\infty}^{\infty} e^{\pm j\theta} e^{-\theta^2/2\sigma_\theta^2} d\theta = \frac{1}{\sqrt{2\pi\sigma_\theta^2}} \int_{-\infty}^{\infty} \cos(\theta) e^{-\theta^2/2\sigma_\theta^2} d\theta + \frac{j}{\sqrt{2\pi\sigma_\theta^2}} \int_{-\infty}^{\infty} \sin(\pm\theta) e^{-\theta^2/2\sigma_\theta^2} d\theta = e^{-\sigma_\theta^2/2}$$

since the value of the imaginary integral is zero. Substituting this result into the expression for average power in (3), the average Uplink Array power is given by

$$\overline{|s(t | \boldsymbol{\theta})|^2}^\theta = P \left( N + \sum_{i=1}^N \sum_{\substack{k=1 \\ k \neq i}}^N \overline{e^{j[\theta_i(t)]}}^\theta \overline{e^{-j[\theta_k(t)]}}^\theta \right) = P \left( N + N(N-1)e^{-\sigma_\theta^2} \right) \quad (4)$$

It is interesting to examine the limiting case of vanishingly small and arbitrarily large phase error variance, namely  $\sigma_\theta^2 \rightarrow 0$  and  $\sigma_\theta^2 \rightarrow \infty$ , which reveal the behavior of combined power both with perfect phasing and with totally random phase:

$$\lim_{\sigma_\theta^2 \rightarrow 0} \overline{|s(t | \boldsymbol{\theta})|^2}^\theta = P \left( N + N(N-1)e^{-\sigma_\theta^2} \Big|_{\sigma_\theta^2 \rightarrow 0} \right) = PN^2 = \max \overline{|s(t | \boldsymbol{\theta})|^2}^\theta$$

$$\lim_{\sigma_\theta^2 \rightarrow \infty} \overline{|s(t | \boldsymbol{\theta})|^2}^\theta = P \left( N + N(N-1)e^{-\sigma_\theta^2} \Big|_{\sigma_\theta^2 \rightarrow \infty} \right) = PN = \min \overline{|s(t | \boldsymbol{\theta})|^2}^\theta$$

We can associate the coefficient  $N$  with the total power at the spacecraft, added non-coherently without any coherent combining gain. The coefficient  $N(N-1)e^{-\sigma_\theta^2}$  can be associated with the coherently combined signal power, which attains its maximum value of  $N(N-1)$  when the phase error variance approaches zero, and disappears as the phase variance approaches infinity, or becomes very large, leaving only the non-coherently added fields.

With perfect phasing such that  $\sigma_\theta^2 \rightarrow 0$ , the combined power at the spacecraft increases by a factor of  $N^2$ , as expected for a coherently phased array since the amplitudes add in this case. With random phase,  $\sigma_\theta^2 \rightarrow \infty$ , the signals combine non-coherently, yielding only the sum of the powers as the lower limit on Uplink Array power: in this case there is only a factor of  $N$  increase in signal power at the spacecraft.

## The General Gaussian Solution

Assume that the phase vector  $\boldsymbol{\theta} = (\theta_1, \theta_2, \dots, \theta_N)$  is a Gaussian random vector with probability density

$$p(\boldsymbol{\theta}) = \frac{\exp[-\frac{1}{2}(\boldsymbol{\theta} - \bar{\boldsymbol{\theta}})\boldsymbol{\Lambda}_\theta^{-1}(\boldsymbol{\theta} - \bar{\boldsymbol{\theta}})^T]}{(2\pi)^{N/2} |\boldsymbol{\Lambda}_\theta|^{1/2}}, \text{ where } \bar{\boldsymbol{\theta}} = (\bar{\theta}_1, \bar{\theta}_2, \dots, \bar{\theta}_N), \boldsymbol{\Lambda}_\theta = E\{(\boldsymbol{\theta} - \bar{\boldsymbol{\theta}})^T(\boldsymbol{\theta} - \bar{\boldsymbol{\theta}})\},$$

$\sigma_{\theta_i}^2 = E(\theta_i - \bar{\theta}_i)^2$ , and  $\lambda_{\theta_{i,k}} = E\{(\theta_i - \bar{\theta}_i)(\theta_k - \bar{\theta}_k)\}$ . For a Gaussian random vector  $\boldsymbol{\theta}$  the characteristic function is defined as [3]  $M_\theta(\mathbf{v}) = E\{\exp[j\mathbf{v}\boldsymbol{\theta}^T]\} = \exp(-\frac{1}{2}\mathbf{v}\boldsymbol{\Lambda}_\theta\mathbf{v}^T + j\mathbf{v}\bar{\boldsymbol{\theta}}^T)$ , which allows writing the expectation of a complex function as  $\overline{e^{j(\theta_i + \theta_k)\theta}} = E\{\exp[j\mathbf{v}\boldsymbol{\theta}^T]\}_{\mathbf{v}=\mathbf{1}} = M_{\theta_{i,k}}(\mathbf{v}=\mathbf{1})$ .

This idea can be generalized to incorporate both positive and negative phases via the transformation  $\boldsymbol{\varphi}^T = \mathbf{A}\boldsymbol{\theta}^T$ , yielding  $M_\varphi(\mathbf{v}) = E\{e^{j\mathbf{v}\boldsymbol{\varphi}^T}\} = E\{e^{j(\mathbf{v}\mathbf{A})\boldsymbol{\theta}^T}\} = \exp(-\frac{1}{2}\mathbf{v}\mathbf{A}\boldsymbol{\Lambda}_\theta\mathbf{A}^T\mathbf{v}^T + j\mathbf{v}\mathbf{A}\bar{\boldsymbol{\theta}}^T)$ . For example, with  $\boldsymbol{\theta}_{i,k} = (\theta_i, \theta_k)$ ,  $\bar{\boldsymbol{\theta}}_{i,k} = (\bar{\theta}_i, \bar{\theta}_k)$ ,  $\mathbf{A} = \text{diag}(1, -1)$ , the expected value of the complex function with phase differences can be expressed compactly as the characteristic function of the

$$\text{transformed variables } \mathbf{A}\boldsymbol{\theta}^T = \begin{bmatrix} 1 & 0 \\ 0 & -1 \end{bmatrix} \begin{bmatrix} \theta_1 \\ \theta_2 \end{bmatrix} = \begin{bmatrix} \theta_1 \\ -\theta_2 \end{bmatrix}, \text{ with } \mathbf{A}\bar{\boldsymbol{\theta}}^T = \begin{bmatrix} 1 & 0 \\ 0 & -1 \end{bmatrix} \begin{bmatrix} \bar{\theta}_1 \\ \bar{\theta}_2 \end{bmatrix} = \begin{bmatrix} \bar{\theta}_1 \\ -\bar{\theta}_2 \end{bmatrix},$$

$$\boldsymbol{\Lambda}_{\theta_{i,k}} = \begin{bmatrix} \sigma_{\theta_i}^2 & \lambda_{\theta_{i,k}} \\ \lambda_{\theta_{k,i}} & \sigma_{\theta_k}^2 \end{bmatrix}, \text{ and } \mathbf{A}\boldsymbol{\Lambda}_{\theta_{i,k}}\mathbf{A}^T = \mathbf{A} \begin{bmatrix} \sigma_{\theta_i}^2 & \lambda_{1,2} \\ \lambda_{1,2} & \sigma_{\theta_2}^2 \end{bmatrix} \mathbf{A}^T = \begin{bmatrix} \sigma_{\theta_i}^2 & -\lambda_{1,2} \\ -\lambda_{1,2} & \sigma_{\theta_2}^2 \end{bmatrix};$$

$$\overline{e^{j(\theta_i - \theta_k)\theta}} = \exp(-\frac{1}{2}\mathbf{v}\mathbf{A}\boldsymbol{\Lambda}_\theta\mathbf{A}^T\mathbf{v}^T + j\mathbf{v}\mathbf{A}\bar{\boldsymbol{\theta}}^T)|_{\mathbf{v}=\mathbf{1}} = \exp[-\frac{1}{2}(\sigma_{\theta_i}^2 + \sigma_{\theta_2}^2 - 2\lambda_{1,2}) + j(\bar{\theta}_1 - \bar{\theta}_2)] = M_{\varphi_{i,k}}(\mathbf{v}=\mathbf{1})$$

With the help of the characteristic function notation, we can now rewrite the average power of the combined signals in the following form:

$$\overline{|s(t|\boldsymbol{\theta})|^2}^\theta = \overline{\left| \sqrt{P} \sum_{i=1}^N e^{j\theta_i(t)} \right|^2}^\theta = P \left( N + \sum_{i=1}^N \sum_{k \neq i}^N \overline{e^{j[\theta_i(t) - \theta_k(t)]}}^\theta \right) = P \left( N + \sum_{i=1}^N \sum_{k \neq i}^N M_{\varphi_{i,k}}(\mathbf{v}=\mathbf{1}) \right)$$

Note that the double sum of characteristic functions contains  $N(N-1)$  terms, which is always an even number: half the terms contain exponents of the form  $j(\bar{\theta}_i - \bar{\theta}_k)$ , the other half contains  $j(\bar{\theta}_k - \bar{\theta}_i)$ .

Therefore, we can decompose the double sum into two separate components:

$$\sum_{i=1}^N \sum_{\substack{k=1 \\ k \neq i}}^N M_{\varphi_{i,k}}(\mathbf{v}=\mathbf{1}) = \sum_{i=1}^{N-1} \sum_{k>i}^N M_{\varphi_{i,k}}(\mathbf{v}=\mathbf{1}) + \sum_{k=1}^{N-1} \sum_{i>k}^N M_{\varphi_{i,k}}(\mathbf{v}=\mathbf{1})$$

Recognizing that  $(\bar{\theta}_k - \bar{\theta}_i) = -(\bar{\theta}_i - \bar{\theta}_k)$  and collecting terms, the double sum of characteristic functions can finally be expressed in terms of the fundamental phase statistics as:

$$\begin{aligned} & \sum_{i=1}^{N-1} \sum_{k>i}^N \exp[-\frac{1}{2}(\sigma_{\theta_i}^2 - 2\lambda_{\theta_{i,k}} + \sigma_{\theta_k}^2) + j(\bar{\theta}_i - \bar{\theta}_k)] + \sum_{k=1}^{N-1} \sum_{i>k}^N \exp[-\frac{1}{2}(\sigma_{\theta_k}^2 - 2\lambda_{\theta_{k,i}} + \sigma_{\theta_i}^2) - j(\bar{\theta}_i - \bar{\theta}_k)] \\ &= 2 \sum_{i=1}^{N-1} \sum_{k>i}^N \exp[-\frac{1}{2}(\sigma_{\theta_i}^2 - 2\lambda_{\theta_{i,k}} + \sigma_{\theta_k}^2)] \cos(\bar{\theta}_i - \bar{\theta}_k) \end{aligned}$$

With the help of this result, we can now express the complete solution for the general Gaussian case, including possible correlations among the phase components as well as non-zero means:

$$\overline{|s(t|\boldsymbol{\theta})|^2}^\theta = P \left( N + \sum_{i=1}^N \sum_{k \neq i}^N M_{\varphi_{i,k}}(\mathbf{v} = \mathbf{1}) \right) = P \left( N + 2 \sum_{i=1}^{N-1} \sum_{k>i}^N \exp[-\frac{1}{2}(\sigma_{\theta_i}^2 + \sigma_{\theta_k}^2 - 2\lambda_{\theta_{i,k}})] \cos(\bar{\theta}_i - \bar{\theta}_k) \right) \quad (6)$$

Having derived the general solution, special cases corresponding to equal mean values, uncorrelated phases, equal variances and even deterministic phase (i.e. the zero-variance case) can be obtained directly by substituting into equation (6). Next, we consider these special cases and obtain explicit expressions for the average combined power for each case:

- 1) Equal Mean Values. When the phases are not zero-mean random variables, but their mean values are the approximately the same, really corresponds to the zero-mean condition as far as combining performance is concerned. This is because signal combining at the spacecraft depends only on phase differences, not absolute phase with respect to some arbitrary reference point in time. Indeed, if we let the mean values be the same in equation (6) the cosine term disappears, and combining efficiency depends only on the variances and covariances among all the pairs:

If  $\bar{\theta}_i = \bar{\theta}_k \quad \forall i, k$  then  $(\bar{\theta}_i - \bar{\theta}_k) = 0$ ,  $M_{\varphi_{i,k}}[\mathbf{v} = \mathbf{1}] = \exp[-\frac{1}{2}(\sigma_{\theta_i}^2 + \sigma_{\theta_k}^2 - 2\lambda_{\theta_{i,k}})]$  and the combined power becomes

$$\overline{|s(t|\boldsymbol{\theta})|^2}^\theta = P \left( N + \sum_{i=1}^N \sum_{\substack{k=1 \\ k \neq i}}^N \exp[-\frac{1}{2}(\sigma_{\theta_k}^2 + \sigma_{\theta_i}^2 - 2\lambda_{\theta_{k,i}})] \right) \quad (7)$$

which depends on the variances and the correlation coefficients, but not the mean values since they have been assumed to be equal, and in this application that is really equivalent to the zero-mean case.

- 2) Uncorrelated Phases: Under the Gaussian assumption, uncorrelated implies independence. Indeed, letting the correlation coefficient approach zero,  $\lambda_{\theta_{i,k}} = E(\theta_i \theta_k) = 0 \quad \forall i, k$ , yields characteristic functions that depend only on the variances:  $M_{\varphi_{i,k}}[\mathbf{v} = \mathbf{1}] = \exp[-\frac{1}{2}(\sigma_{\theta_i}^2 + \sigma_{\theta_k}^2)]$ . Substituting into the expression for the average combined power, we obtain

$$\overline{|s(t|\boldsymbol{\theta})|^2}^\theta = P \left( N + \sum_{i=1}^N \sum_{\substack{k=1 \\ k \neq i}}^N \exp[-\frac{1}{2}(\sigma_{\theta_k}^2 + \sigma_{\theta_i}^2)] \right) \quad (8)$$

where the correlation coefficients and means have disappeared, and the combined power depends only on the variances and the number of antennas in the array.

- 3) Equal Variances: When the variances are equal,  $\sigma_{\theta_i}^2 = \sigma_{\theta_k}^2 = \sigma_\theta^2 \quad \forall i, k$ , but the phases are uncorrelated and equal-mean or zero-mean, the characteristic function depends only on the common variance  $\sigma_\theta^2$ :  $M_{\phi_{i,k}}[\nu = \mathbf{1}] = \exp[-\sigma_\theta^2]$ . Summing the components yields the same expression as obtained previously using the “classical” derivation:

$$\overline{|s(t|\boldsymbol{\theta})|^2}^\theta = P \left( N + \sum_{i=1}^N \sum_{\substack{k=1 \\ k \neq i}}^N \exp[-\sigma_\theta^2] \right) = P(N + N(N-1)e^{-\sigma_\theta^2}) \quad (9)$$

As before, the limiting cases imply a gain of  $N^2$  for perfectly phased antennas, and a gain of  $N$  for the incoherent case, as expected from the structure of the far-field pattern and from conservation of energy.

- 4) Deterministic Case: Finally, we consider the zero-variance case which implies non-random but unequal phases, where the correlation coefficients are all zero:  $\sigma_{\theta_i}^2 = \sigma_{\theta_k}^2 = \lambda_{\theta_{i,k}} = 0 \quad \forall i, k$ . Substituting for the characteristic function yields  $M_{\phi_{i,k}}(\omega) = 2 \cos[\omega(\bar{\theta}_i - \bar{\theta}_k)]$ , and the combined power now depends only on the pairwise phase differences:

$$\overline{|s(t|\boldsymbol{\theta})|^2}^\theta = P \left( N + 2 \sum_{i=1}^{N-1} \sum_{k>i}^N \cos(\bar{\theta}_i - \bar{\theta}_k) \right) \quad (10)$$

The summation cannot be simplified any further without explicit knowledge of the mean phase vector  $\bar{\boldsymbol{\theta}}$ , except for the equal mean value case considered earlier.

## More Realistic Tikhonov Phase Model

Let’s reconsider the equal-variance, zero-mean, statistically independent phase vector case, but this time assuming a more realistic Tikhonov (or von Mises) probability density for the individual phase. This density is defined over the interval  $[-\pi, \pi)$ , hence the infinite-variance case corresponds to a uniform density of level  $1/2\pi$  over this interval, as opposed to the Gaussian approximation whose level approaches zero over the infinite interval. The Tikhonov probability density is defined as

$p(\theta_i) = \frac{e^{\rho_\theta \cos \theta_i}}{2\pi I_0(\rho_\theta)}$ ,  $-\pi < \theta_i \leq \pi$ , where  $\rho_\theta$  is proportional to  $\sigma_\theta^{-2}$ . The behavior of the Tikhonov density as a function of  $\theta$ , for various parameters from zero to 20, is shown in Fig. 4, over the interval  $[-\pi, \pi)$ .

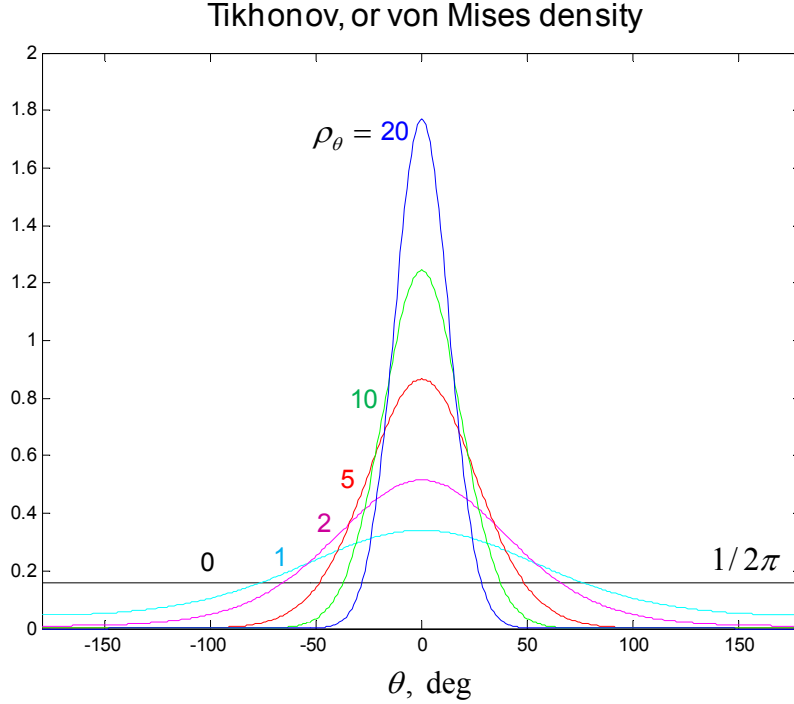


Figure 4. Tikhonov (or von Mises) probability density, for various values of the parameter  $\rho_\theta$ .

We again start with the definition of combined power and make use of the assumed statistical independence  $\theta_i, \theta_k$ :

$$\overline{|s(t|\mathbf{\theta})|^2}^\theta = \overline{\left| \sqrt{P} \sum_{i=1}^N e^{j\theta_i(t)} \right|^2}^\theta = P \left( N + \overline{\sum_{i=1}^N \sum_{\substack{k=1 \\ k \neq i}}^N e^{j[\theta_i(t)]} e^{-j[\theta_k(t)]}}^\theta \right) = P \left( N + \sum_{i=1}^N \sum_{\substack{k=1 \\ k \neq i}}^N \overline{e^{j[\theta_i(t)]} e^{-j[\theta_k(t)]}}^\theta \right) \quad (11)$$

This time, however, we average with respect to the Tikhonov density instead of the Gaussian density as in the previous derivation [3]:

$$I_0(\rho_\theta) \overline{e^{\pm j\theta}} = \frac{1}{2\pi} \int_{-\pi}^{\pi} e^{\pm j\theta} e^{\rho_\theta \cos(\theta)} d\theta = \frac{1}{2\pi} \int_{-\pi}^{\pi} \cos(\theta) e^{\rho_\theta \cos(\theta)} d\theta + \frac{j}{2\pi} \int_{-\pi}^{\pi} \sin(\pm\theta) e^{\rho_\theta \cos(\theta)} d\theta = I_1(\rho_\theta)$$

Note that the argument of the imaginary integral is odd, yielding zero over the symmetric interval. The average Uplink Array power now becomes

$$\overline{|s(t|\boldsymbol{\theta})|^2}^\theta = P \left( N + \sum_{i=1}^N \sum_{\substack{k=1 \\ k \neq i}}^N e^{jI\theta_i(t)} e^{-jI\theta_k(t)} \right) = P \left( N + N(N-1) \left[ \frac{I_1(\rho_\theta)}{I_0(\rho_\theta)} \right]^2 \right) \quad (12)$$

The difference between the Tikhonov and Gaussian case is that  $e^{-\sigma_\theta^2}$  is replaced by  $[I_1(\rho_\theta)/I_0(\rho_\theta)]^2$ . This leads to a slightly different behavior of combined power for the Tikhonov case, as shown for the case of a two-antenna array,  $N = 2$ , in Fig. 5 when  $\lambda_\theta = 0$ , however the limiting cases remain the same:

$$\begin{aligned} \lim_{\rho_\theta \rightarrow \infty} \overline{|s(t|\boldsymbol{\theta})|^2}^\theta &= P(N + N(N-1)[I_1(\rho_\theta)/I_0(\rho_\theta)]^2 |_{\rho_\theta \rightarrow \infty}) = PN^2 = \max \overline{|s(t|\boldsymbol{\theta})|^2}^\theta \\ \lim_{\rho_\theta \rightarrow 0} \overline{|s(t|\boldsymbol{\theta})|^2}^\theta &= P(N + N(N-1)[I_1(\rho_\theta)/I_0(\rho_\theta)]^2 |_{\rho_\theta \rightarrow 0}) = PN = \min \overline{|s(t|\boldsymbol{\theta})|^2}^\theta \end{aligned}$$

We again note that the coefficient  $N$  represents the non-coherently added signal fields. The coefficient  $N(N-1)[I_1(\rho_\theta)/I_0(\rho_\theta)]^2$  represents the coherently combined signal power, again attaining its maximum value of  $N(N-1)$  when the parameter  $\rho_\theta$  (corresponding to the inverse of the phase error variance) approaches infinity, and disappearing as  $\rho_\theta$  approaches zero.

For the special case of two and three antenna Uplink Arrays,  $N=2$  and 3, as practiced in the DSN with the antennas of the Apollo complex, it is reasonable to assume that the phases are equally-correlated and of equal variance, in which case the average power at the spacecraft reduces to the following expression:

$$\overline{|s(t|\boldsymbol{\theta})|^2}^\theta = P \left( N + \sum_{i=1}^N \sum_{\substack{k=1 \\ k \neq i}}^N \exp[-\frac{1}{2}(\sigma_{\theta_k}^2 + \sigma_{\theta_i}^2 - 2\lambda_{\theta_{k,i}})] \right) = P(N + N(N-1)\exp[-(\sigma_\theta^2 - \lambda_\theta)]) \quad (13)$$

These cases are illustrated in Fig. 5 for the case of two and three antenna Uplink Arrays with equal baselines and common correlation coefficients of  $\lambda_\theta = 0, 0.5$  and  $0.9$ .

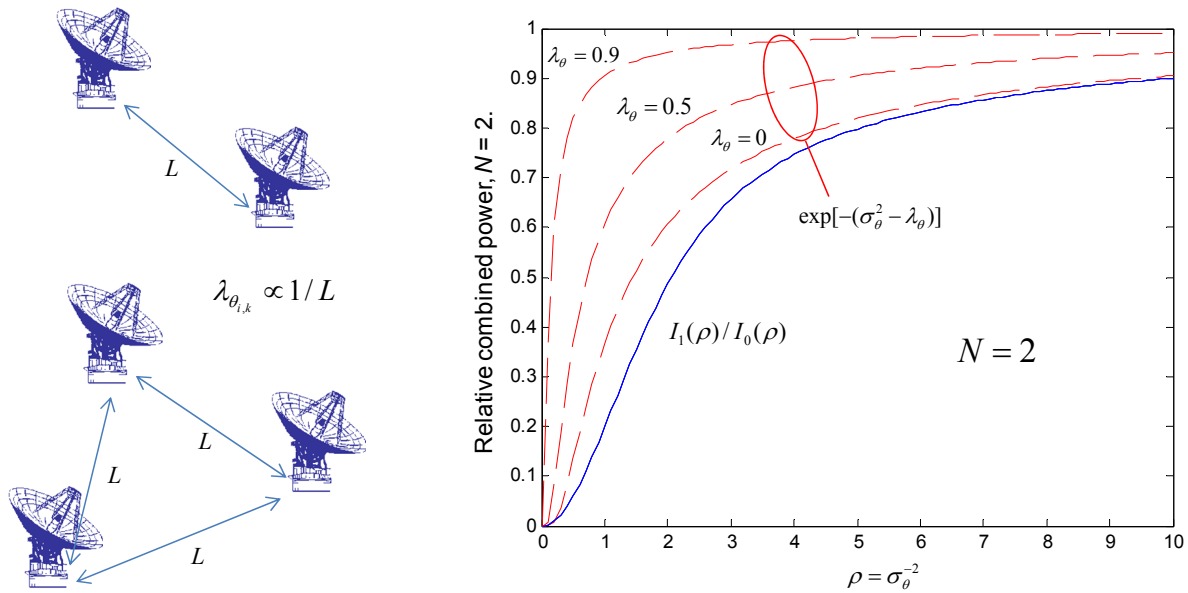


**Fig. 5. a) Definition of symmetrical two and three antenna array baselines; b) comparison of relative combined powers with the uncorrelated Tikhonov and Gaussian densities, and the behavior of correlated phases with the Gaussian assumption for two and three antenna Uplink Arrays.**

### 3. Uplink Array Model for Modulated Signals

Although combining of unmodulated carriers is useful for determining relative Doppler between the ground and a distant spacecraft, the main purpose of uplink arraying is to increase the useful communication range or data-rate at the spacecraft. Modulation is required for the transmission of information, but with several array antennas transmitting from different geographical locations the signals reach the spacecraft with different delays, even if the carrier phases have been properly compensated. The reason is that unmodulated carriers can be phased up even if there are many integer carrier wavelengths of error between them, provided the residual “fractional wavelength” errors have been compensated out. However, with modulated carriers the much slower modulating waveforms also must be lined up, which implies compensating the integer number of wavelengths as well. But delay compensation is subject to error, much like carrier phase compensation, leading to degraded fidelity in the combined signal and ultimately limiting the data rate. We begin by constructing a mathematical model suitable for representing the delay-compensated array signal at the spacecraft, and first determining the impact of deterministic errors, followed by statistical analysis to quantify average performance in the presence of random delay errors.

Consider the delay model for the modulation shown in Fig. 6: the delay to the spacecraft is calculated and applied at the  $i$ -th antenna, however a residual delay error may remain due to unmodeled error sources.

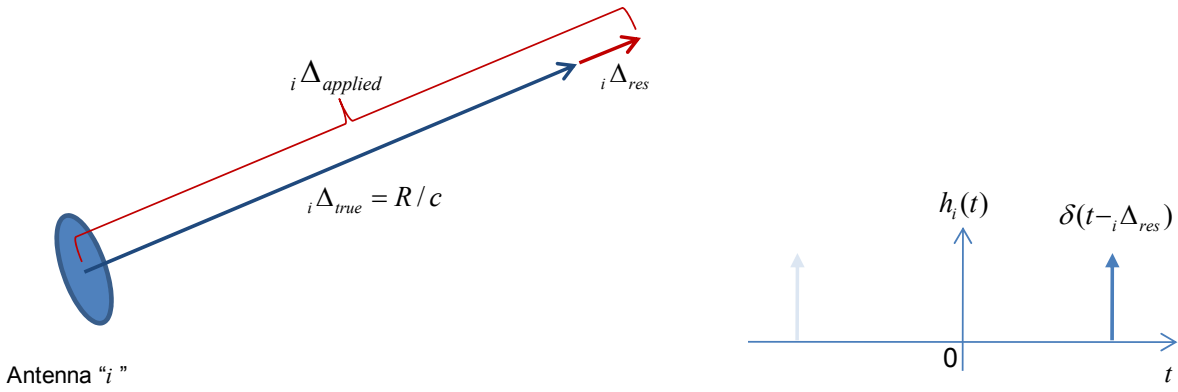


**Figure 6. a) Physical model of true delay, applied delay, and residual delay for the  $i$ -th antenna; b) impulse response model of residual delay.**

The impulse response of the residual delay for the  $i$ -th antenna is modeled as the difference of the true and applied delays, expressed mathematically in terms of ideal delta-functions as:

$${}_i h_{total}(t) = \delta(t - {}_i\Delta_{applied}) = \delta[t - ({}_i\Delta_{true} + {}_i\Delta_{res})]; \quad {}_i\Delta_{res} \equiv {}_i\Delta_{applied} - {}_i\Delta_{true}; \quad h_i(t) \equiv \delta(t - {}_i\Delta_{res});$$

We assume that each antenna has associated with it a residual delay, which may or may not be independent of the other delays. The consequence of applying different residual delays to the modulation can be seen in Fig. 7a, where two waveforms with different residual delays arrive at the spacecraft at slightly different times, hence do not add perfectly but lead to distortion in the sum-signal, as shown in Fig. 7b.

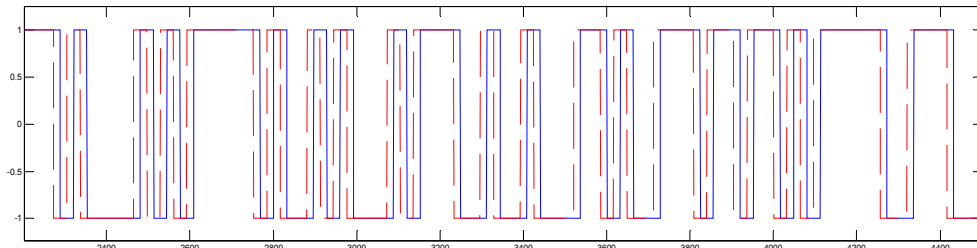


**Figure 7a) Example of received  $\pm 1$  data sequence (solid blue), and its delayed version (red dash)**

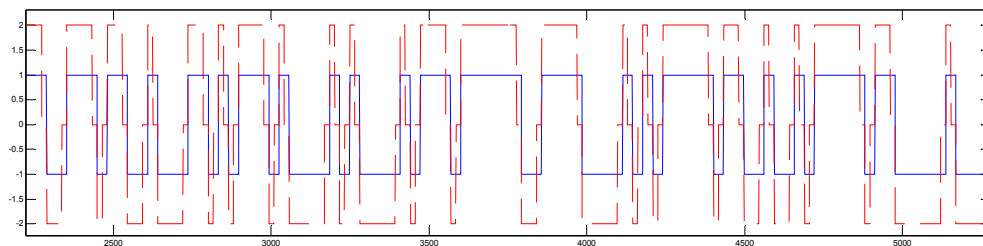


**Figure 7b) Sum of  $\pm 1$  data sequence and its delayed version, with  $\Delta = -T/2$ ;  $T = 32$  samples**

At the spacecraft, delayed versions of the received signals add with generally different delays, characterized by a delay vector  $\Delta = (\Delta_1, \Delta_2, \dots, \Delta_N)$ , which can be expressed as the convolution of the signal waveform  $s_0(t)$  with the impulse response of the Uplink Array channel,  $h_\Sigma(t)$  :

$$s(t | \Delta) = \sum_i s_i(t - \Delta_i) = \sum_i s_0(t) * h_i(t) = s_0(t) * \sum_i h_i(t) \equiv s_0(t) * h_\Sigma(t) \quad (14)$$

The transfer function of the Uplink Array channel is the Fourier Transform of the channel impulse response, which can be expressed as  $H_\Sigma(j\omega) \equiv \mathcal{F}\{h_\Sigma(t)\} = \sum_i \mathcal{F}\{h_i(t)\} = \sum_i H_i(j\omega)$ . Fourier transforming the impulse response  $h_i(t) = \delta(t - \Delta_i)$  yields  $H(j\omega | \Delta_i) = \exp(-j\omega \Delta_i)$ , hence we obtain the channel impulse response  $H_\Sigma(j\omega | \Delta) = \sum_i \exp(-j\omega \Delta_i)$ . Writing the sum of the delayed signal components as  $s(t | \Delta) = \sum_i s_i(t - \Delta_i) = s_0(t) * h_\Sigma(t)$  and Fourier transforming, it follows that  $\mathcal{F}\{s(t | \Delta)\} = \mathcal{F}\{s_0(t)\} H_\Sigma(j\omega | \Delta)$ . Invoking the classical definition of power spectral density as the expected value of the squared magnitude of the signal's Fourier transform, we define the average power spectral density of a randomly modulated signal as  $P_s(\omega) = E |S_0(\omega)|^2 \equiv E |\mathcal{F}\{s_0(t)\}|^2$ .

The periodogram of the combined signal conditioned on a residual delay vector  $\Delta = (\Delta_1, \Delta_2, \dots, \Delta_N)$  is the squared magnitude of its Fourier transform [5]:  $I(\omega | \Delta) \equiv |\mathcal{F}\{s(t | \Delta)\}|^2 = |S_0(\omega)|^2 |H_\Sigma(j\omega)|^2$ . The variance of the periodogram at any frequency is proportional to "spectral level squared", hence this estimator of the power spectrum is not consistent:  $\text{var}[I_0(\omega)] \propto [I_0(\omega)]^2$  where  $I_0(\omega) = |S_0(\omega)|^2$ .

Estimator variance can be reduced by averaging, yielding greatly improved estimator performance:

$$\overline{I_0(\omega)}^L = \sum_{l=1}^L |S_{0,l}(\omega)|^2 \equiv \overline{|S_0(\omega)|^2}^L; \quad \rightarrow \quad \text{var}[\overline{I_0(\omega)}^L] \propto \frac{1}{L} \text{var}[I_0(\omega)].$$

Figs 8 a) and b) demonstrate the improvement afforded by averaging a hundred periodograms, thus reducing the standard deviation of the spectral estimate by a factor of ten, as evident in Fig. 8b. In the limit as  $N \rightarrow \infty$  the averaged periodogram approaches the expected value of the squared magnitude of the signal Fourier transform, thus providing a useful way to verify the theoretical results via simulation. In the following examples, the theoretical results will be supported by simulation, where 100 sample-functions of random binary data-sequences will be Fourier transformed and averaged to reduce the variance.

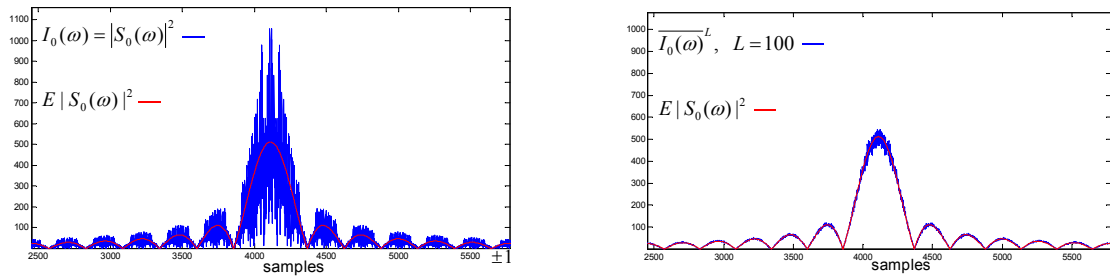


**Fig. 8. a) Theoretical power spectrum of BPSK modulation, and single realization of its periodogram; b) average of 100 periodograms, demonstrating the reduction of estimator variance.**

The following example helps to illustrate these points. Consider an Uplink Array channel with two antennas,  $N=2$ , residual delays  $\Delta = (\Delta_1 = 0, \Delta_2 = 0.5T)$ , and  $\sigma_{\Delta_i}^2 = \sigma_{\Delta_k}^2 = \lambda_{\Delta_{i,k}} = 0$ . The channel transfer function for the two-element uplink array can be written directly as

$$|H_{\Sigma}(j\omega | \Delta_1, \Delta_2)|^2 = 2 + 2 \sum_{i=1}^1 \sum_{k>i}^2 \cos[\omega(\Delta_2 - \Delta_1)] = 2 + 2 \cos[\omega(\Delta_2 - \Delta_1)] \quad (15)$$

while the averaged periodogram for the two-element uplink array becomes

$$\overline{I(\omega | \Delta_1, \Delta_2)}^L = |S_0(\omega)|^2 |H_{\Sigma}(j\omega)|^2 \propto \frac{\sin^2(\omega T / 2)}{(\omega T / 2)^2} (2 + 2 \cos[\omega(\Delta_2 - \Delta_1)]),$$

when the delays are

deterministic constants. The power spectrum of the original signal and the periodogram of the two-element uplink array with half-symbol delay difference (averaged over a hundred realizations) is shown in Fig. 9, clearly illustrating the impact of the sinusoidal component in equation (15).

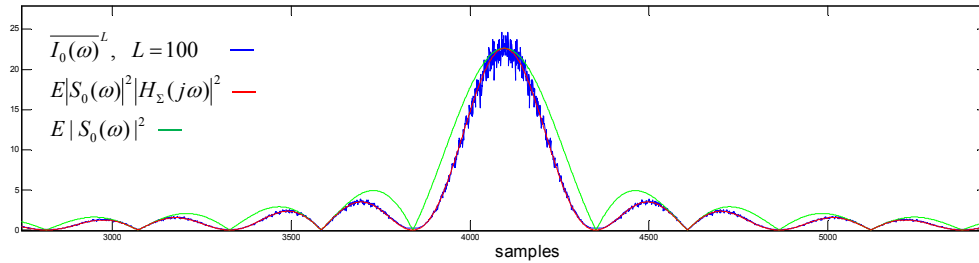


**Fig. 9. Power spectrum of the original signal, spectrum of two-element combined signal with half-symbol delay difference, and averaged periodogram simulation confirming theory.**

## Conventional Derivation of Delay-Averaged Power Spectrum

Following the format of the previous section for deriving the average power of an unmodulated uplink array signals, we start with a conventional derivation of the delay-averaged power spectrum for modulated signals assuming statistically independent, zero-mean, equal-variance Normally distributed random delays. Since delays are not limited to a range of values, as was the case with phase, the Gaussian assumption is perfectly valid for delays with arbitrary variance, not only for small variance as was the case for phase. Letting  $\Delta_i$  and  $\Delta_k$  be SI  $\forall i \neq k$ , and let  $p(\Delta) = \frac{1}{\sqrt{2\pi\sigma_{\Delta}^2}} e^{-\Delta^2/2\sigma_{\Delta}^2}$ , where  $\sigma_{\Delta}^2$  is the common variance, we can express the periodogram conditioned on the delay vector and the number of sample-functions to be averaged,  $L$ , as:

$$\overline{I(\omega | \Delta)}^{L,\Delta} = \overline{|S_0(\omega)|^2 \left| \sum_{i=1}^N e^{j\omega\Delta_i(t)} \right|^2}^\Delta = \overline{|S_0(\omega)|^2}^{L,\Delta} \left( N + \sum_{i=1}^N \sum_{\substack{k=1 \\ k \neq i}}^N \overline{e^{j\omega\Delta_i(t)} e^{-j\omega\Delta_k(t)}}^\Delta \right) = \overline{|S_0(\omega)|^2}^{L,\Delta} \left( N + \sum_{i=1}^N \sum_{\substack{k=1 \\ k \neq i}}^N \overline{e^{j\omega\Delta_i(t)} e^{-j\omega\Delta_k(t)}}^\Delta \right) \quad (16)$$

Averaging with respect the Gaussian density for delay yields [3]

$$\overline{e^{\pm j\omega\Delta}} = \frac{1}{\sqrt{2\pi\sigma_\Delta^2}} \int_{-\infty}^{\infty} e^{\pm j\omega\Delta} e^{-\Delta^2/2\sigma_\Delta^2} d\Delta = \frac{1}{\sqrt{2\pi\sigma_\Delta^2}} \int_{-\infty}^{\infty} \cos(\omega\Delta) e^{-\Delta^2/2\sigma_\Delta^2} d\Delta + \frac{j}{\sqrt{2\pi\sigma_\Delta^2}} \int_{-\infty}^{\infty} \sin(\pm\omega\Delta) e^{-\Delta^2/2\sigma_\Delta^2} d\Delta = e^{-\omega^2\sigma_\Delta^2/2}$$

where we argue, as before, that the integral of the imaginary term is zero since the sine is an odd function of delay. Substituting into equation (16) yields an estimate of the average Uplink Array power spectrum as

$$P(\omega) = \lim_{L \rightarrow \infty} \overline{I(\omega | \Delta)}^{L,\Delta} = \lim_{L \rightarrow \infty} \overline{|S_0(\omega)|^2}^{L,\Delta} \left( N + \sum_{i=1}^N \sum_{\substack{k=1 \\ k \neq i}}^N \overline{e^{j\omega\Delta_k} e^{-j\omega\Delta_i}}^\Delta \right) = |S_0(\omega)|^2 \left( N + N(N-1) e^{-\omega^2\sigma_\Delta^2} \right) \quad (17)$$

where we have implicitly replaced the averaging of  $L$  samples of the signal spectrum with random modulation, with the expected value of the function  $|S_0(\omega)|^2$  as  $L$  approaches infinity.

## General Derivation of Delay-Averaged Power Spectrum

We now assume that  $\Delta$  is a vector with generalized Gaussian probability density function  $p(\Delta) = \exp[-\frac{1}{2}(\Delta - \bar{\Delta})\Lambda_\Delta^{-1}(\Delta - \bar{\Delta})^T] / (2\pi)^{N/2} |\Lambda_\Delta|^{1/2}$  and write the delay and sample-function averaged periodogram in terms of the two-element characteristic function as

$$\begin{aligned} \overline{I(\omega | \Delta)}^{L,\Delta} &\equiv \overline{\mathcal{F}\{s(t | \Delta)\}^2}^{L,\Delta} = \overline{|S_0(\omega)|^2 |H_\Sigma(j\omega | \Delta)|^2}^\Delta = \overline{|S_0(\omega)|^2 \sum_{i=1}^N \sum_{k=1}^N e^{j\omega(\Delta_k - \Delta_i)}}^\Delta \\ &= \overline{|S_0(\omega)|^2}^{L,\Delta} \left( N + \sum_{i=1}^N \sum_{\substack{k=1 \\ k \neq i}}^N \overline{e^{j\omega(\Delta_k - \Delta_i)}}^\Delta \right) = \overline{|S_0(\omega)|^2}^{L,\Delta} \left( N + \sum_{i=1}^N \sum_{\substack{k=1 \\ k \neq i}}^N M_{\Delta_{i,k}}(\omega) \right) \end{aligned} \quad (18)$$

with  $M_{\Delta_{i,k}}(\omega) = \exp(-\frac{1}{2}\omega \mathbf{A}^T \Lambda_\Delta \mathbf{A} \omega + j\omega \mathbf{A} \bar{\Delta}^T)$ ,  $\omega = (\omega_1, \omega_2) |_{\omega_1=\omega_2=\omega}$ ,  $\Delta = (\Delta_i, \Delta_k)$ ,

$$\bar{\Delta} = (\bar{\Delta}_i, \bar{\Delta}_k), \quad \mathbf{A} = \text{diag}(1, -1), \quad \Lambda_{\Delta_{i,k}} = \begin{bmatrix} \sigma_{\Delta_i}^2 & \gamma_{i,k} \\ \gamma_{i,k} & \sigma_{\Delta_k}^2 \end{bmatrix}, \quad \text{where } \gamma_{i,k} = E\{(\Delta_i - \bar{\Delta}_i)(\Delta_k - \bar{\Delta}_k)\}.$$

Substituting for  $\mathbf{A}$ ,  $\Lambda_\Delta$ , and  $\bar{\Delta}$ , in equation (18) we obtain the two-component characteristic function

$M_{\Delta_i,k}(\boldsymbol{\omega}) = \exp(-\frac{1}{2}\boldsymbol{\omega}\mathbf{A}^T\boldsymbol{\Lambda}_\Delta\mathbf{A}\boldsymbol{\omega} + j\boldsymbol{\omega}\mathbf{A}\bar{\Delta}^T) = \exp[-\frac{1}{2}(\sigma_{\Delta_i}^2 + \sigma_{\Delta_k}^2 - 2\gamma_{i,k})\omega^2 + j\omega(\bar{\Delta}_i - \bar{\Delta}_k)]$ , which in turn yields the delay averaged power spectrum as:

$$P_s(\omega) = \lim_{L \rightarrow \infty} \overline{|S_0(\omega)|^2}^L \left( N + \sum_{i=1}^N \sum_{\substack{k=1 \\ k \neq i}}^N M_{\Delta_i,k}(\boldsymbol{\omega}) \right) = E|S_0(\omega)|^2 \left( N + 2 \sum_{i=1}^{N-1} \sum_{k>i}^N \exp[-\frac{1}{2}\omega^2(\sigma_{\Delta_i}^2 - 2\lambda_{\Delta_i,k} + \sigma_{\Delta_k}^2)] \cos[\omega(\bar{\Delta}_i - \bar{\Delta}_k)] \right) \quad (19)$$

where we replaced  $\lim_{L \rightarrow \infty} \overline{|S_0(\omega)|^2}^L$  with  $E|S_0(\omega)|^2$  for simplicity (equivalent to assuming that  $L \rightarrow \infty$ ).

Several special cases follow directly from this general result:

- 1) **Equal Mean Values:** If  $\bar{\Delta}_i = \bar{\Delta}_k \quad \forall i, k$  then  $(\bar{\Delta}_i - \bar{\Delta}_k) = 0$ , and the two-element characteristic function follows as  $M_{\Delta_i,k}(\boldsymbol{\omega})|_{\omega_1=\omega_2=\omega} = \exp[-\frac{1}{2}(\sigma_{\Delta_i}^2 + \sigma_{\Delta_k}^2 - 2\lambda_{\Delta_i,k})]$ . Substituting into equation (19) yields  $P_s(\omega) = E|S_0(\omega)|^2 \left( N + 2 \sum_{i=1}^{N-1} \sum_{k>i}^N \exp[-\frac{1}{2}\omega^2(\sigma_{\Delta_k}^2 + \sigma_{\Delta_i}^2 - 2\lambda_{\Delta_k,i})] \right)$ .
- 2) **Uncorrelated Delays:** If  $\lambda_{\Delta_i,k} = E(\Delta_i\Delta_k) = 0 \quad \forall i, k$  in addition to equal mean-values, we obtain the pairwise characteristic function  $M_{\Delta_i,k}(\omega) = \exp[-\frac{1}{2}\omega^2(\sigma_{\Delta_i}^2 + \sigma_{\Delta_k}^2)]$  and direct substitution yields  $P_s(\omega) = E|S_0(\omega)|^2 \left( N + 2 \sum_{i=1}^{N-1} \sum_{k>i}^N \exp[-\frac{1}{2}\omega^2(\sigma_{\Delta_k}^2 + \sigma_{\Delta_i}^2)] \right)$
- 3) **Equal Variances:** If  $\sigma_{\Delta_i}^2 = \sigma_{\Delta_k}^2 = \sigma_\Delta^2 \quad \forall i, k$  then  $M_{\Delta_i,k}(\omega) = \exp[-\omega^2\sigma_\Delta^2]$  and  $P_s(\omega) = E|S_0(\omega)|^2 \left( N + 2 \sum_{i=1}^{N-1} \sum_{k>i}^N \exp[-\omega^2\sigma_\Delta^2] \right) = E|S_0(\omega)|^2 \left( N + N(N-1)e^{-\omega^2\sigma_\Delta^2} \right)$
- 4) **Deterministic Delays:** This is the limiting case as we let the variance approach zero. With  $\sigma_{\Delta_i}^2 = \sigma_{\Delta_k}^2 = \lambda_{\Delta_i,k} = 0$ , the characteristic function becomes  $M_{\Delta_i,k}(\omega) = 2 \cos[\omega(\bar{\Delta}_i - \bar{\Delta}_k)]$  yielding the averaged power spectrum  $P_s(\omega) = E|S_0(\omega)|^2 \left( N + 2 \sum_{i=1}^{N-1} \sum_{k>i}^N \cos[\omega(\bar{\Delta}_i - \bar{\Delta}_k)] \right)$ .

Note that these results are fundamentally different from the unmodulated carrier case obtained earlier, because  $e^{-\sigma_\theta^2}$  is not a function of frequency, but a constant, hence approaches the constant “one” as  $\sigma_\theta^2$  approaches zero, and the constant “zero” as  $\sigma_\theta^2$  becomes arbitrarily large. By contrast,  $e^{-\omega^2\sigma_\Delta^2}$  is a function of frequency, approaching the constant “one” for all frequencies as  $\sigma_\Delta^2$  approaches zero, but becoming a narrow Gaussian function of frequency as  $\sigma_\Delta^2$  increases: however, its peak value remains “one” regardless of how great  $\sigma_\Delta^2$  becomes. Therefore, the coherent coefficient  $N(N-1)e^{-\omega^2\sigma_\Delta^2}$  reduces

the bandwidth of the coherent component as  $\sigma_{\Delta}^2$  increases, but leaves the peak value (at zero frequency) unaltered.

It is interesting to examine these results for a range of “root-mean-square” (rms) delays, from rms delays much smaller to much greater than a symbol duration. Since large-variance cases are difficult to simulate, we rely on our analytically derived results, namely equation (19), to evaluate this behavior. Assuming uncorrelated, equal-variance and equal-mean delays, and letting the delay variance change according to  $\sigma_{\Delta}^2 = 100T^2 * 8^{-(k-1)}$ , yields the following standard deviations:  $\sigma_{\Delta} = 10T, 3.54T, 1.25T, 0.442T, 0.156T$  as  $k$  varies from 1 to 5, corresponding to the power spectral densities shown in Fig. 10.

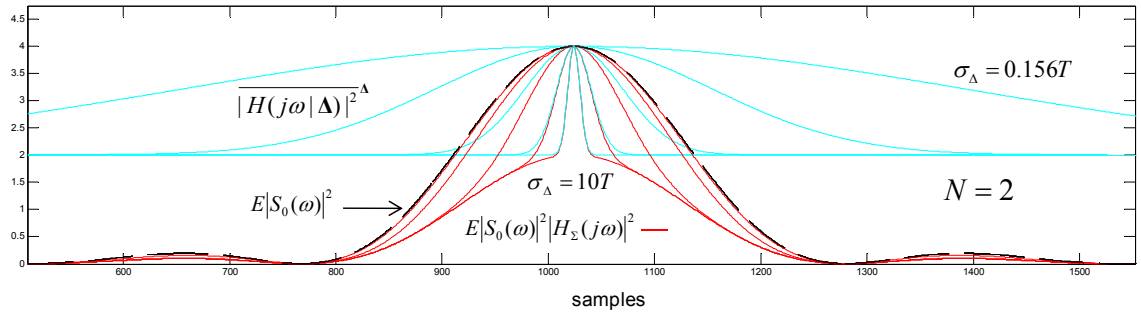


**Fig. 10. Impact of random delay error on the power spectral density of Uplink Array signals, for a wide range of delay error standard deviations.**

In Fig. 10, the blue curves are the averaged channel transfer functions, the dashed black curve is the signal power spectrum, and the red curves are the power spectra of the combined signal at the spacecraft. It is immediately obvious from Fig. 10 that for small standard deviations the impact of delay errors on the power spectrum of the combined signal is minimal, but a much greater impact is evident for large delay errors, due to the extreme narrowing of the peak of the channel transfer function. However, this only affects the coherently added component, which account for the extra 3 dB gain over the incoherently added signal powers under ideal conditions. Recall that the coherent part is multiplied by  $N(N-1)$  and the non-coherent part by  $N$ : for  $N=2$  both of these coefficients are 2, which accounts for the 3 dB gain of coherent over non-coherent combining for a two-antenna uplink array. For larger values of  $N$  these coefficient values change, with greater power going to the coherent component as  $N$  increases.

It can be seen that as the delay-error variance becomes arbitrarily great, the upper half of the power spectrum corresponding to the coherently added components becomes extremely narrow, and eventually no signal power whatsoever remains in the coherent part of the power spectrum. Thus, for the two-antenna case we are considering, the total power, which is the integral of the power spectral density over frequency, approaches four times the individual antenna power in the case of perfect combining, but only twice the individual signal powers for the case of non-coherent combining. These results confirms the earlier limiting-case behavior of  $N^2$  and  $N$ , respectively, for coherent and noncoherent combining, but clarifies the manner in which the power spectrum of the combined signal changes. The severe narrowing of the coherent part indicates that high-rate data throughput at this power level is not possible in the

presence of large delay errors, however data throughput at the original rate should be possible albeit with reduced power levels by means of a more complicated receiver that selects the data-streams by synchronizing to each delay separately, which could be accomplished by correlating with known frame markers, for example, or by using partially decoded symbols in a feedback configuration, then adds the outputs via equal-ratio combining if the array elements are identical, or weighted combining in case different size and power antennas are used. The processing for non-coherent combining is similar to the processing currently used for Doppler delay calibration via the Moon-Bounce technique [6] and planetary radar imaging, as described in [2]. In other words, there is always a component of the power spectrum that retains the full bandwidth of the original signal, but the gain over a single antenna is  $N$ , instead of  $N^2$  as in the fully coherent case. Although the examples in Fig. 10 assumed a two-element uplink array, the general structure of the uplink array spectrum remains the same for larger values of  $N$ , with the non-coherent full-bandwidth portion providing a gain of  $N$  over a single antenna, and the coherent portion providing a gain of  $N(N-1)$  over a single antenna at full bandwidth if the delay errors are small, and reduced bandwidth as the delay errors exceed the symbol-duration. We never lose by using more antennas to transmit the same data to the spacecraft, but the greatest possible gain is realized only when the signals are combined coherently at the spacecraft.

The total power within the power spectrum for  $N=2$  was determined as a function of  $k$ , which corresponds to delay-error variance according to the above equation, and shown in Fig. 11.

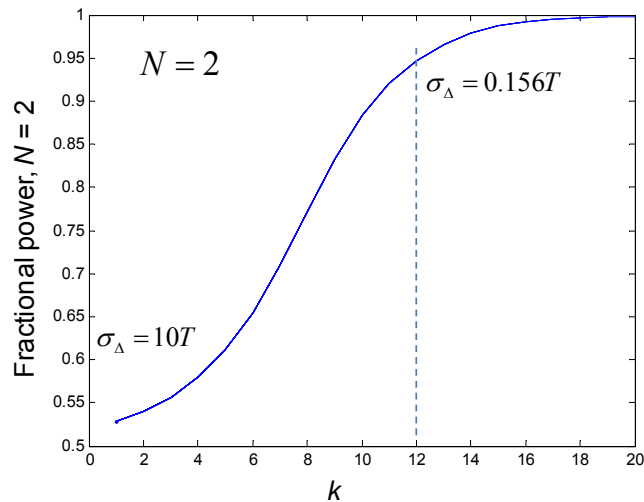


**Fig. 11. Fractional power in two-antenna uplink array signals, as a function of  $k$ .**

Note that for large rms delay deviations (small  $k$ ) the fractional power approaches 0.5, corresponding to the incoherent combining case with  $N=2$ , while for small rms deviations the fractional power approaches one, as expected with coherent combining.

Finally, we consider the general case of simultaneous delay and phase errors, as typically occurs in practical uplink arraying applications. The assumption of independence is reasonable, since phase compensation and delay compensation typically take place in different parts of the signal generation and

distribution system. We start by writing the signal at the spacecraft, now conditioned on both a phase and delay error vector, as  $s(t | \boldsymbol{\theta}, \boldsymbol{\Delta}) = \sqrt{P} \sum_i e^{j\theta_i} s_0(t - \Delta_i) = \sqrt{P} s_0(t) * \sum_{i=1}^N e^{j\theta_i} \delta(t - \Delta_i) = \sqrt{P} s_0(t) * \tilde{h}_\Sigma(t)$ ,

where  $H_\Sigma(j\omega | \boldsymbol{\theta}, \boldsymbol{\Delta}) \equiv \sum_i \mathcal{F}\{h_i(t | \theta_i, \Delta_i)\} = \sum_i \tilde{H}_i(j\omega | \theta_i, \Delta_i) = \sum_{i=1}^N e^{j\theta_i} e^{-j\omega\Delta_i} = \sum_{i=1}^N e^{-j(\omega\Delta_i - \theta_i)}$  is the

joint transfer function, incorporating both phase and delay errors. Since  $\boldsymbol{\theta}$  and  $\boldsymbol{\Delta}$  are assumed to be SI, the respective exponential components factor, and we can average them separately inside the joint transfer function. Averaging with respect to the delay errors first, we obtain:

$$\overline{|\tilde{H}_\Sigma(j\omega | \boldsymbol{\theta}, \boldsymbol{\Delta})|^2}^\Delta = N + \sum_{i=1}^N \sum_{\substack{k=1 \\ k \neq i}}^N e^{j(\theta_i - \theta_k)} \overline{e^{-j\omega(\Delta_i - \Delta_k)}}^\Delta = N + \sum_{i=1}^N \sum_{\substack{k=1 \\ k \neq i}}^N e^{j(\theta_i - \theta_k)} M_{\Delta_{i,k}}(\boldsymbol{\omega}) \quad (20)$$

Next, we average this partial result with respect to the phase errors, obtaining:

$$\overline{|\tilde{H}_\Sigma(j\omega | \boldsymbol{\theta}, \boldsymbol{\Delta})|^2}^{\Delta, \boldsymbol{\theta}} = N + \sum_{i=1}^N \sum_{\substack{k=1 \\ k \neq i}}^N \overline{e^{j(\theta_i - \theta_k)}}^{\boldsymbol{\theta}} M_{\Delta_{i,k}}(\boldsymbol{\omega}) = N + \sum_{i=1}^N \sum_{\substack{k=1 \\ k \neq i}}^N M_{\Phi_{i,k}}(\mathbf{v} = \mathbf{1}) M_{\Delta_{i,k}}(\boldsymbol{\omega}) \quad (21)$$

Substituting the phase and time averaged transfer function into the expression for the power spectral density, finally yields:

$$P_s(\omega) = P |S_0(\omega)|^2 \left( N + 2 \sum_{i=1}^{N-1} \sum_{k>i}^N e^{-\frac{1}{2}(\sigma_{\theta_i}^2 + \sigma_{\theta_k}^2 - 2\lambda_{\theta_{i,k}})} e^{-\frac{1}{2}\omega^2(\sigma_{\Delta_i}^2 - 2\lambda_{\Delta_{i,k}} + \sigma_{\Delta_k}^2)} \cos(\bar{\theta}_i - \bar{\theta}_k) \cos[\omega(\bar{\Delta}_i - \bar{\Delta}_k)] \right) \quad (22)$$

The various special cases corresponding to equal mean values and correlated random variables follow directly from equation (22) as before, hence need not be re-examined here. However, there is one special case that is worth examining: the case of equal-variance, equal-mean (or zero-mean), uncorrelated random phase and delay vectors. In this case, the power spectral density reduces to:

$$P_s(\omega) = P |S_0(\omega)|^2 \left( N + N(N-1)e^{-\sigma_\theta^2} e^{-\omega^2\sigma_\Delta^2} \right) \quad (23)$$

which is in a form similar to the previous carrier phase error results. It can be seen from equation (23) that both phase and delay errors impact the combined power at the spacecraft, but in a fundamentally different way: random phase errors reduce the total power in the coherent component as the phase-error variance increases, but leave the bandwidth of the coherent component unaltered; random delay errors, on the other hand, leave the peak value of the coherent component unaltered, but reduce its bandwidth as the delay error variance increases. Both error sources leave the peak value and bandwidth of the non-coherent component unaltered, providing a gain of  $N$  over a single antenna at the spacecraft. This implies that high-speed data at the original design rate can still be processed and decoded at the spacecraft, even in the absence of significant combining gain, but a different receiver processing is called for, and the fidelity of the data may be impacted due to the loss of coherently combined signal power.

## 4. Summary and Conclusions

The impact of carrier phase and modulation delay errors on the efficiency of Uplink Array combining has been determined in a very general form, including phase and delay correlations among the array elements as well as non-zero mean values, by application of the characteristic function of Gaussian random vectors. The Gaussian model is eminently reasonable for random delay errors due to slowly varying pathlength errors, and also applicable to random carrier phase vectors provided the rms values are small compared to a wavelength. An improved solution has also been developed for phase vectors with arbitrarily large phase variance using the Tikhonov probability density, but restricted to statistically independent phase residuals. The dependence of the power spectrum of the combined signal has been determined, and shown to be composed of two distinct components with generally different bandwidths, depending on the variance of the delay errors. For phase and delay errors small compared to a symbol-duration the power spectrum essentially retains  $N^2$  array gain with full bandwidth, allowing for the transmission of information at the highest possible data-rate. The results derived in this paper are significant since communications engineers will now be able to evaluate the impact of any combination of random or non-random phase and delay errors on Uplink Array performance, enabling optimized designs for Uplink Array systems in the future.

**Acknowledgment:** This research was carried out at the Jet Propulsion Laboratory, California Institute of Technology, under a contract with the National Aeronautics and Space Administration.

## 5. References

- [1] V. Vilnrotter, D. Lee, T. Cornish, P. Tsao, L. Paal, V. Jamnejad, "Uplink Array Concept Demonstration with the EPOXI Spacecraft," IEEE Aerospace Conference, Big Sky, MN, March 2009.
- [2] V. Vilnrotter, P. Tsao, D. Lee, T. Cornish, J. Jao, M. Slade, 'Planetary Radar Imaging with the Deep-Space Network's 34 meter Uplink Array," IEEE Aerospace Conference, Big Sky, MN, March 2011.
- [3] Abramowitz and Stegun, *Handbook of Mathematical Functions*, Dover, New York, 1970.
- [4] Wozencraft and Jacobs, *Principles of Communications Engineering*, John Wiley and Sons, New York, 1965.
- [5] Oppenheim and Schaffer, *Digital Signal Processing*, Prentice-Hall, Englewood Cliffs, NJ, 1975.
- [6] V. Vilnrotter, P. Tsao, D. Lee, T. Cornish, L. Paal, "Uplink Array Calibration via Lunar Doppler-Delay Imaging," IEEE Aerospace Conference, Big Sky, MN, March 2010.